Zheng Hong-guang*, Yao Li-jiang and Xu Heng

Effect of Two Kinds of Refiners on the Solidification Structure and Property of Invar Alloy

Abstract: The solidification structure of two 500 g cylindrical ingots of Fe-36Ni invar alloy, which were melted in a carbon tube furnace and cast adding Ce and Zr-Ti refiners respectively, were investigated. The results showed that the grain size became smaller. With the increase of refiner content, the ratio of equiaxed grains of ingot increased and the equiaxed grain size decreased. As for the 100 kg flat ingot, which was melted in a vacuum induction furnace and cast with Ce and Zr-Ti refiners respectively, the situation was different slightly. When adding Ce the dendritic grain diameter of the flat ingot became finer and the equiaxed grain ratio remained low; however, the mechanical property deteriorated. While adding Zr-Ti complex refiners, the solidification structure of the alloy was improved dramatically. Therefore, the mechanical properties at room temperature of as-cast flat ingots were improved. Furthermore, its high temperature ductility range expanded and the expansion coefficient of its hot-rolling plate remained almost the same.

Keywords: Fe-36Ni, invar alloy, Ce, Zr-Ti, solidification structure, ductility

***Corresponding author: Zheng Hong-guang:** Baosteel R & D Institute, Shanghai 201900, China. E-mail: zhenghg828@gmail.com
Yao Li-jiang, Xu Heng: Baosteel Special Materials Co. Ltd, Shanghai 200940, China

1 Introduction

In recent years, Fe-36Ni invar alloy has attracted extensive attention for its very low expansion coefficient. The product application has expanded to many fields, such as the traditional precision instrument industry, and to other uses, such as electronic application and special structure materials [1–3]. The production line of invar alloy traditionally consists of ingot casting, electroslag remelting and forging. However, this traditional process produced lower yield, higher cost and lower efficiency. In recent years, Fe-36Ni alloy can be produced by the vertical slab continuous caster, but the Fe-36Ni slab tends to crack in the hot rolling process. Based on the slab macrostructure, it can be seen that the initial austenite grain size of the slab is coarse, which may have great influence on the hot ductility of slab. It is therefore necessary to find a way to improve the solidification structure of invar alloy and make clear the relationship of its solidification structure and ductility. Yang Xiao-hua has reported that Ce and Nb can refine the solidification structure of Fe-43Ni alloy under the water cooling condition [4–5]. Suito has found that Ce and Ti can refine the solidification structure of Fe-10Ni alloy [6]. However, researches on how to improve the solidification structure of Fe-36Ni alloy and clarity on the relationship of its solidification structure and hot ductility have not been reported. This paper focuses on the effect of rare earth Ce and Zr-Ti complex refiners on the solidification structure and property of Fe-36Ni invar alloy.

2 Experimental procedures

2.1 Experiment in a corundum crucible

The chemical composition (wt.%) of Fe-36Ni alloy used in this study is as follows: 0.013C, 0.17Si, 0.30Mn, 0.008P, 0.001S, 36.22Ni and the remainder Fe. The refiners added are rare earth Ce, sponge titanium and Zr powder.

Approximately 0.5 kg of alloy with and without refiners was smelted in a carbon tube furnace protected by argon at a temperature of 1530 °C. The refiner was inserted into the liquid alloy after deoxidization, and then the molten alloy was refined for 1 min. Subsequently, the molten alloy was poured into a Φ37 mm mould at 1460 °C, and then air cooled to room temperature.

The alloy ingots were sectioned along the transverse section and the samples were then ground, polished and chemically etched. The etchant used for macrostructure: 4 g picric acid + 100 ml C_2H_5OH + 3 ml HCl; the etchant for microstructure: ferric chloride alcohol saturated solution. The average grain size and the equiaxed grain fraction were determined according to the ASTM standard [7]. The types of inclusions in the alloys were observed and detected by SEM/EDS.

2.2 Experiment in a vacuum induction furnace

Experimental materials used are as follows: pure iron, pure nickel, ferrosilicon and aluminum. The refiners added are misch rare earth, sponge titanium and Zr powder. Because the misch rare earth consists of a great amount of Ce and a small part of La, only the content of Ce in the alloy was examined for the convenience.

Fe-36Ni invar alloy with and without refiners were smelted in a vacuum induction furnace at 1600 °C. The refiner was added into the molten alloy after melting, and when the temperature and composition were uniform, the molten alloy was cast into 100 kg flat ingots at a pouring temperature of 1530–1550 °C under vacuum conditions.

Samples with a transverse dimension of 228 × 105 mm and cut from the flat ingots were prepared for macrostructure investigation, the etchant for macrostructure: 30%HCl solution. The equiaxed grain fraction was determined by the area calculation method.

Samples obtained were perpendicular to the columnar crystal growth direction, and the sampling position ranged from 2 cm to 3.5 cm from the edge of the flat ingots. Then samples were made for room temperature tensile strength testing in order to measure the yield strength and tensile strength on a SCL103 tensile testing machine, and samples with dimensions of Φ10 × 120 mm were machined to test the reduction of area in the temperature range of 800–1300 °C with an interval of 50 °C on a Gleeble thermal simulation testing machine.

The flat ingot was hot-rolled to a 15 mm plate at an initial rolling temperature of 1200 °C and a finishing temperature of 900–1050 °C, and then finally air cooled to room temperature. Samples cut from the plate with dimensions of Φ6.0 × 24.5 mm were first heat-treated at a temperature of 840 °C, and then maintained at a temperature of 315 °C for an hour and finally air cooled to room temperature. The expansion coefficient was determined on a DIL402C thermal expansion instrument.

3 Experimental result

3.1 Solidification structure

Fig. 1 illustrates macrostructures without and with refiners. The corresponding characteristic parameters of the solidification structure are shown in Table 1. It can be seen that the solidification structures of the alloys were well improved with the addition of Ce or Zr-Ti refiners, resulting in the columnar grain of solidification structure to be remarkably shorter and thinner. With the increase of refiner content, the ratio of equiaxed grains increased and

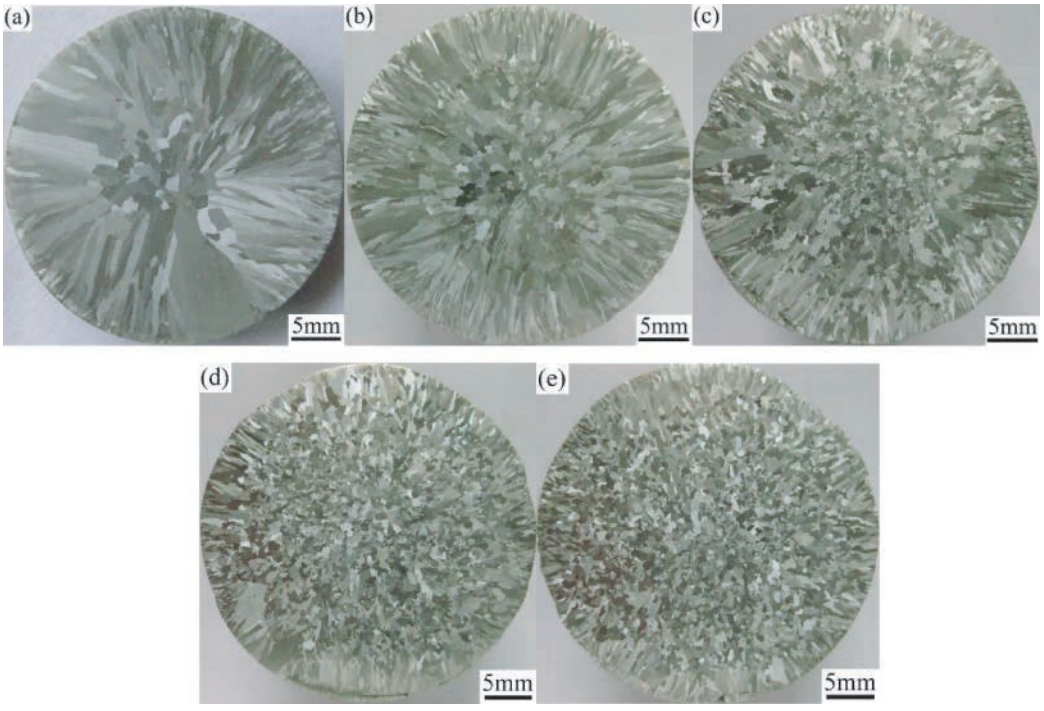

Fig. 1: Macrostructures of cylindrical ingots of Fe-36Ni alloy

Table 1: Relationship of refiner content and characteristic parameters of solidification structures

Sample no.	Ce content (%)	Zr content (%)	Ti content (%)	Equiaxed grain ratio (%)	Average equiaxed grain size (mm)
a	–	–	–	8	3.212
b	0.16	–	–	33	1.623
c	0.22	–	–	56	1.135
d	–	0.026	0.038	66	0.935
e	–	0.048	0.061	71	0.841

Table 2: Relationship of refiner content and characteristic parameters of solidification structures

Sample no.	Refiner content (%)	Equiaxed grains ratio (%)	Columnar grains
a	–	13	coarse
b	0.15%Ce	0	thin
c	0.05%Zr-0.13%Ti	36	shorter, thinner

the equiaxed grain size decreased. Although the content of Zr-Ti complex refiner was lower, the effect of improving the solidification structure was better.

Fig. 2 shows macrostructures of ingots without and with refiners melted in a vacuum induction furnace. The corresponding characteristic parameters of the solidification structure are shown in Table 2. It can be seen from Fig. 2 that the columnar grain became obviously thinner due to the addition of 0.15%Ce. The solidification structure of the alloy was well improved with the addition of Zr-Ti refiner, and the ratio of equiaxed grains increased to 36%.

3.2 Results of room temperature tensile test

The results of room temperature tensile test are shown in Fig. 3. The tensile strength and the yield strength of flat ingots without the addition of refiners are 338 MPa and 205 MPa, respectively. However, the tensile strength of flat ingots with the addition of 0.15%Ce decreased to 42 MPa, and the mechanical properties at room temperature deteriorated sharply. The tensile strength and the yield strength of samples with the addition of 0.05%Zr-0.13%Ti increased 44 MPa and 32 MPa respectively, and the mechanical properties at room temperature improved a little.

3.3 Results of high temperature tensile test

The reduction of area of flat ingots is shown in Fig. 4. When prepared, samples with the addition of 0.15%Ce frequently fractured, so the reduction of area couldn't be obtained. Moreover, the flat ingot cracked during the hot rolling process, as shown in Fig. 5. Therefore, the high temperature ductility of the flat ingot deteriorated sharply.

It is believed that the content of the Ce reached to 0.15% in this study, excessive rare earth not only polluted the alloy, but also reacted with Fe and Ni to form brittle intermetallic phases (Fe-Ni-Ce-La), which scattered on

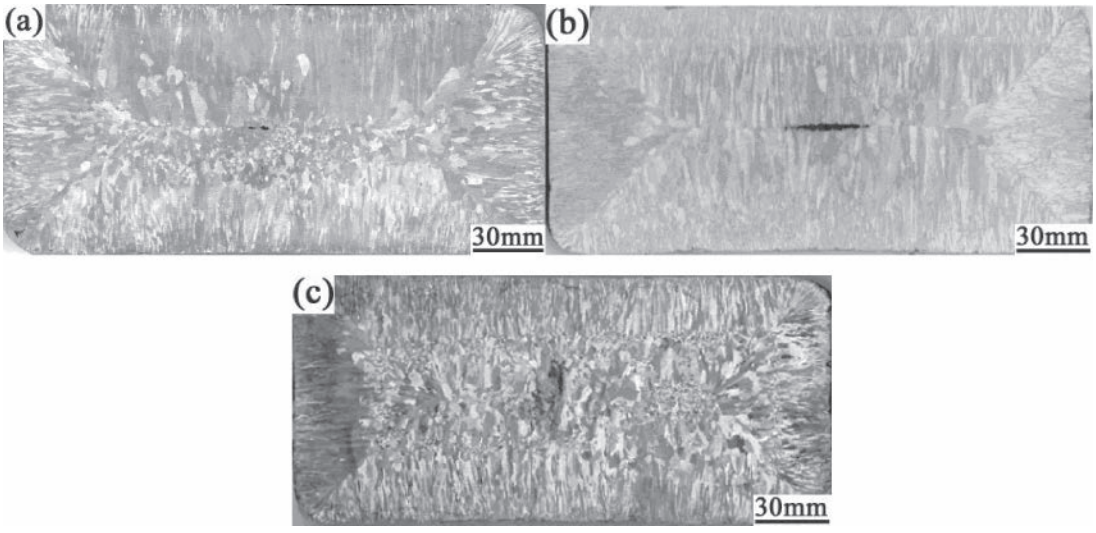

Fig. 2: Macrostructures of flat ingots of Fe-36Ni alloy

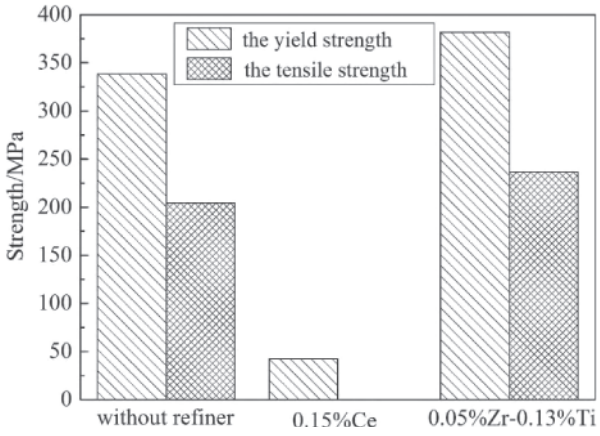

Fig. 3: Mechanical properties at room temperature of flat ingots

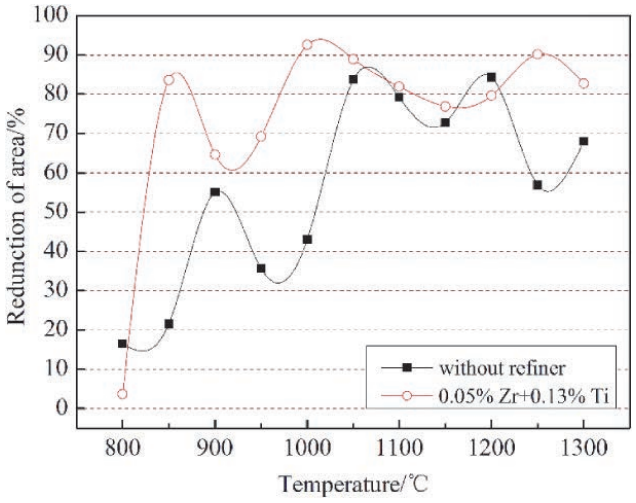

Fig. 4: Relationship of reduction of area vs temperature

Fig. 5: The cracked flat ingot in hot rolling process

grain boundaries. The typical example is shown in Fig. 6 and the compositions are given in Table 3. The brittle intermetallic phases not only weaken the grain boundary binding force, but also hindered the movement of the grain boundaries in the hot rolling process. Therefore, formation of the brittle intermetallic phase on grain boundaries leads to deteriorated mechanical property.

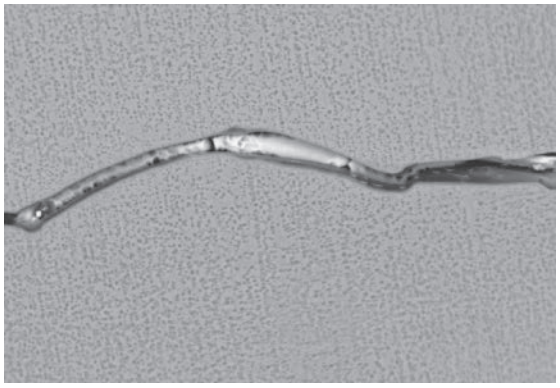

Fig. 6: SEM images of rare earth intermetallic compounds at grain boundaries

Table 3: EDS results of rare earth intermetallic compounds (%, mass fraction)

Fe	Ni	Ce	La
16.20	55.83	21.79	6.17

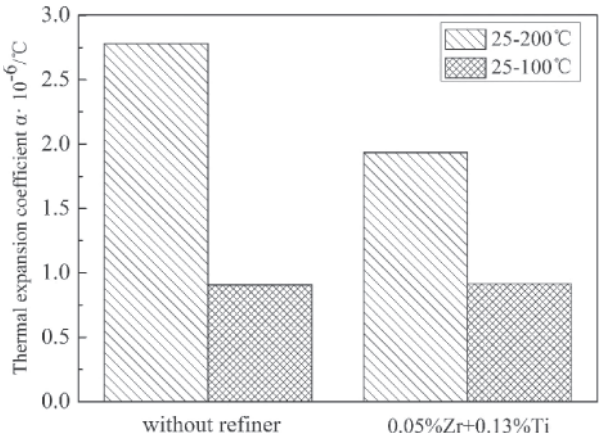

Fig. 7: Results of the thermal expansion coefficient

However, the reduction of area of the flat ingot was higher than that without the addition of refiners, and the high temperature ductility range expanded nearly 200 °C due to 0.05%Zr-0.13%Ti. Therefore, the high temperature ductility of the flat ingot is well improved.

3.4 Results of thermal expansion coefficient test

The expansion coefficient results of the hot rolling plate are shown in Fig. 7. The flat ingot with the addition of 0.15%Ce cracked during the hot rolling process, so the expansion coefficient couldn't be obtained.

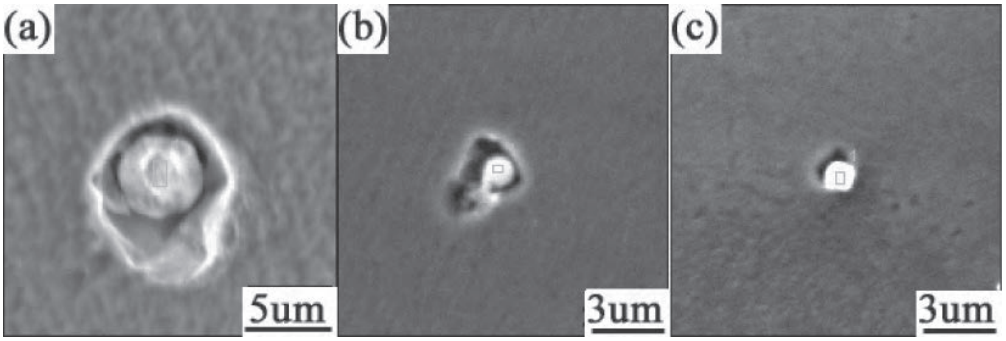

Fig. 8: SEM images of the particle inside an equiaxed grain

The variation law of average expansion coefficient of 25–200 °C is not consistent with that of 25–100 °C. With the addition of 0.05%Zr-0.13%Ti, the average expansion coefficient of 25–200 °C decreased 30%, but the average expansion coefficient of 25–100 °C slightly increased, up to 0.915×10^{-6}/°C. In the invar alloy process, there is a criteria that the average expansion coefficient of 25–100 °C must be less than 1.0×10^{-6}/°C. Therefore, it can be seen that the thermal expansion coefficient of the alloy meets the production requirement with 0.05%Zr-0.13%Ti refiners.

4 Discussion

The solidification structures of the alloys were improved with the addition of Ce or Zr-Ti refiners. The refinement mechanism is discussed below.

Due to different refiners, different types of inclusions formed. With the addition of Ce or Zr-Ti refiners, plenty of Ce_2O_3, and ZrO_2, ZrO_2-Ti_2O_3 particles formed respectively and would mostly act as the cores of equiaxed grains. Typical examples are shown in Fig. 8. The compositions of typical inclusions are given in Table 4. The melting point of Ce_2O_3, ZrO_2 and Ti_2O_3 are 1690 °C, 2680 °C and 1900 °C, respectively. At smelting temperature, they were solid phase particles and may serve as the core of heterogeneous nucleation during the metal solidification process.

According to Turnbull and Vonnegut [8], the nucleating agent could benefit the microstructure of the ingot, but the two following conditions are necessary: (a) there are high-melting point particles in liquid, which provide an interface of the heterogeneous nucleation, (b) the lattice misfit of low-index surfaces between high-melting phase particles and matrix metal should be lower.

The crystallographic data of Ce_2O_3, ZrO_2, Ti_2O_3 and the matrix of Fe-36Ni invar alloy are given in Table 5 [9–12].

Based on the work by Bramfitt [13], the two-dimensional lattice misfit mathematical model is as follows:

$$\delta_{(hkl)_n}^{(hkl)_s} = \sum_{i=1}^{3} \left(\left| \frac{\left(d_{[uvw]_s^i} \cos\theta \right) - d_{[uvw]_n^i}}{d_{[uvw]_n^i}} \right| \times 100 \right) \Big/ 3 \qquad (1)$$

where δ is the lattice misfit of the two interfaces, $(hkl)_s$ is the low index plane of the substrate, $[uvw]_s$ is the low index direction in $(hkl)_s$, $(hkl)_n$ is the low index plane in the nucleated solid, $[uvw]_n$ is the low index direction in $(hkl)_n$, $d_{[uvw]s}$ and $d_{[uvw]n}$ are the atomic spacing along $[uvw]_s$ and $[uvw]_n$, θ is the angle between $[uvw]_s$ and $[uvw]_n$. The smaller the θ, the lower the δ, and the easier the nucleation during the metal solidification process.

According to Table 5 and Eq. (1), the lattice misfit between Ce_2O_3, ZrO_2, Ti_2O_3 and the matrix of Fe-36Ni invar

Table 4: EDS results of the particle inside equiaxed grains (%, mass fraction)

Element	O	Ce	Zr	Ti	Fe	Ni
a	13.42	80.34	–	–	4.78	1.37
b	16.77	–	38.38	–	23.20	11.65
c	9.96	–	45.61	2.58	27.66	14.19

Table 5: Crystallographic date of effective nucleating agents and the matrix of Fe-36Ni invar alloy

Nucleate particle	Crystal class	Lattice parameters (10^{-10}m) (25 °C)		Lattice parameters (10^{-10}m) (1430 °C)	
		a_0	c_0	a_{01}	c_{01}
Ce_2O_3	Hexagon	3.889	6.054	3.394	–
ZrO_2	$P4_2/nmc$	–	–	3.653	5.297
Ti_2O_3	Corundum-type	–	–	5.125	–
Fe-36Ni	Cubic	3.64	3.64	3.681	3.681

Table 6: The planar misfit between Ce_2O_3 and Fe-36Ni invar alloy

Ce_2O_3//Fe-36Ni	$(hkl)_s$	$(hkl)_n$	$d_{[uvw]s}$	$d_{[uvw]n}$	θ	δ
(0001) Ce_2O_3//	$[\bar{1}2\bar{1}0]$	[010]	3.935	3.681	0	6.21%
(001) Fe-36Ni	$[\bar{2}110]$	[012]	7.870	8.229	3.43	
	$[\bar{1}010]$	[001]	6.816	7.36	0	
(0001) Ce_2O_3//	$[\bar{1}2\bar{1}0]$	$[00\bar{1}]$	3.935	3.681	0	20.28%
(110) Fe-36Ni	$[\bar{2}1\bar{1}0]$	$[\bar{1}1\bar{1}]$	7.870	6.374	5.26	
	$[\bar{1}010]$	$[\bar{1}10]$	6.816	5.204	0	
(0001) Ce_2O_3//	$[\bar{1}2\bar{1}0]$	$[\bar{1}10]$	3.935	2.602	0	51.23%
(111) Fe-36Ni	$[\bar{1}100]$	$[\bar{2}11]$	6.816	4507	0	
	$[\bar{2}110]$	$[\bar{1}01]$	3.935	2.602	0	

Table 7: The planar misfit between ZrO_2 and Fe-36Ni invar alloy

ZrO_2//Fe-36Ni	$(hkl)_s$	$(hkl)_n$	$d_{[uvw]s}$	$d_{[uvw]n}$	θ	δ
(001) ZrO_2//	[010]	[010]	3.653	3.681	0	0.77%
(001) Fe-36Ni	$[\bar{1}10]$	$[\bar{1}10]$	5.165	5.206	0	
	$[\bar{1}00]$	$[\bar{1}00]$	3.653	3.681	0	
(001) ZrO_2//	[010]	$[00\bar{1}]$	3.653	3.681	0	18.56%
(110) Fe-36Ni	$[\bar{1}10]$	$[\bar{1}1\bar{2}]$	5.165	4.508	5.26	
	$[\bar{1}00]$	$[\bar{1}10]$	3.653	2.603	0	
(001) ZrO_2//	[010]	$[\bar{1}10]$	3.653	2.603	0	21.15%
(111) Fe-36Ni	$[\bar{1}10]$	$[\bar{2}11]$	5.165	5.206	15	
	$[\bar{1}00]$	$[\bar{1}01]$	3.653	4.508	0	

Table 8: The planar misfit between Ti_2O_3 and Fe-36Ni invar alloy

Ti_2O_3//Fe-36Ni	$(hkl)_s$	$(hkl)_n$	$d_{[uvw]s}$	$d_{[uvw]n}$	θ	δ
(0001) Ti_2O_3//	$[\bar{1}2\bar{1}0]$	[010]	5.125	3.681	0	27.4%
(001) Fe-36Ni	$[\bar{2}110]$	$[\bar{1}10]$	10.25	8.23	5.91	
	$[\bar{1}010]$	$[\bar{1}00]$	8.876	7.34	0	
(0001) Ti_2O_3//	$[\bar{1}2\bar{1}0]$	$[00\bar{1}]$	5.125	3.681	0	23.45%
(110) Fe-36Ni	$[\bar{2}110]$	$[\bar{3}3\bar{2}]$	10.25	8.633	4.76	
	$[\bar{1}010]$	$[\bar{1}10]$	8.876	7.805	0	
(0001) Ti_2O_3//	$[\bar{1}2\bar{1}0]$	$[\bar{1}10]$	5.125	5.20	0	1.52%
(111) Fe-36Ni	$[\bar{1}100]$	$[\bar{2}11]$	8.877	9.041	0	
	$[\bar{2}110]$	$[\bar{1}01]$	5.125	5.20	0	

alloy have been calculated, which are listed in Table 6, Table 7 and Table 8. It can be seen that the lattice misfit between the face (0001) of Ce_2O_3 and the face (001) of Fe-36Ni invar alloy is 6.21%, the lattice misfit between the face (001) of ZrO_2 and the face (001) of Fe-36Ni invar alloy is 0.77%, the lattice misfit between the face (0001) of Ti_2O_3 and the face (111) of Fe-36Ni invar alloy is 1.52%.

According to Bramfitt [13], $\delta < 6\%$ is the best condition for nucleation, while $\delta = 6\%–12\%$ is also good, and $\delta > 12\%$ is not as good for heterogeneous nucleation. Ce_2O_3, ZrO_2, Ti_2O_3 have high-melting points and the lattice misfits between them and Fe-36Ni invar alloy are also low. Therefore, Ce_2O_3, ZrO_2 and ZrO_2-Ti_2O_3 particles could serve as the core of heterogeneous nucleation and refine the solidification structure of the alloy.

The experimental results of the cylindrical ingots differed from those of the flat ingots with the same refiner, the reason may be as follows: (1) the casting temperature of the former was lower than that of the latter, (2) the mass of the cylindrical ingot weighed just 500 g, so its cooling speed was higher than that of the latter. It is well known that the solidification structure can be improved by lower casting temperature and higher cooling speed. Therefore, the differences above were the comprehensive function of the casting temperature and the cooling speed.

5 Conclusions

1. The solidification structure of cylindrical ingots with the addition Ce or Zr-Ti complex refiners, were well improved, and the ratio of equiaxed grains of ingot increased and the equiaxed grain size decreased with the increase of the refiner content.
2. The dendritic grain diameter of the flat ingot with the addition of Ce, became finer, while the equiaxed grain ratio remained low and the mechanical property deteriorated.
3. The solidification structure of the flat ingot with the addition of Zr-Ti complex refiners, became dramatically finer, and the mechanical properties at room temperature of as-cast flat ingots were improved, while the high temperature ductility range expanded and the expansion coefficient of its hot-rolling plate remained almost the same.

Received: August 1, 2012. Accepted: January 6, 2013.

References

[1] Y. Zhao, Y. S. Sato, H. Kokawa, A. Wu. Microstructure and properties of friction stir welded high strength Fe-36wt%Ni alloy. Materials Science and Engineering A, 2011, 528(25–26): 7768–7773.

[2] B. K. Jasthi, W. J. Arbegast, S. M. Howard. Thermal expansion coefficient and mechanical properties of friction stir welded invar (Fe-36%Ni). Journal of Materials Engineering and Performance, 2009, 18(7): 925–934.

[3] J. Liu. Application and development of low expansion alloys. Metallic Functional Materials, 2007, 14(5): 33–37.
[4] X. H. Yang, W. Q. Chen, Z. Q. Hao. Effect of Ce on the solidification structure of Fe-Ni base invar expansion alloys. Journal of University of Science and Technology Beijing, 2009, 31(7): 867–870.
[5] X. H. Yang, W. Q. Chen, S. Q. Yuan. Effect of Nb metamorphic disposal on solidification structure of Fe-Ni base invar expansion alloy. Journal of Xi'an University of Architecture and Technology, 2009, 41(11): 136–140.
[6] H. Suito, H. Ohta, S. Morioka. Refinement of solidification microstructure and austenite grain by fine inclusion particles. ISIJ International, 2006, 46(6): 840–846.
[7] American National Standards Institute. Annual Book of ASTM Standard, 1977: 207–238.
[8] D. Turnbull, R. Vonnegut. Grain refining of superalloy and its alloys using inoculants. Ind. Eng. Chem., 1952, 44: 1292–1297.
[9] The Metal Department of Sun Yat-Sen University. The Manual of Rare Earth Physical Chemistry. Beijing: Metallurgy Industry Press, 1978: 41.
[10] R. Kohlhaas, Ph. Dünner, N. Schmitz-Pranghe. The temperature-dependence of the lattice parameters of iron, cobalt, and nickel in the high temperature range. Z. Angew. Phys., 1967, 23 (4): 245–249.
[11] P. Aldebert, J. Traverse. Structure and ionic mobility of zirconia at high temperature. Journal of the American Ceramic Society, 1985, 68(1) : 34–40.
[12] C. E. Rice, W. R. Robinson. High-temperature crystal chemistry of Ti_2O_3: structural changes accompanying the semiconductor-metal transition. Acta Crystallogr. B, 1977, 33: 1342–1348.
[13] B. L. Branfitt. The effect of carbide and nitride additions on the heterogeneous nucleation behavior of liquid iron. Metallurgical Transactions, 1970, 7(1): 1987–1995.